Science of the Total Environment 832 (2022) 154847

Contents lists available at ScienceDirect

Science of the Total Environment

journal homepage: www.elsevier.com/locate/scitotenv

Potential obesogenic effects of TBBPA and its alternatives TBBPS and TCBPA revealed by metabolic perturbations in human hepatoma cells

Yunjiang Yu [a,*], Chaojie Hao [a,b], Mingdeng Xiang [a], Jinglin Tian [c], Hongxuan Kuang [a], Zhenchi Li [a,*]

[a] State Environmental Protection Key Laboratory of Environmental Pollution Health Risk Assessment, South China Institute of Environmental Sciences, Ministry of Ecology and Environment, Guangzhou 510655, China
[b] School of Public Health, China Medical University, Liaoning 110122, China
[c] Chemistry Department, Hong Kong Baptist University, Hongkong 999077, China

HIGHLIGHTS

- TBBPA, TBBPS, and TCBPA induced significant metabolic changes in HepG2 cells.
- Glycerophospholipid and fatty acyl were perturbated by the TBBPS at 0.1 μmol/L.
- TBBPS and TCBPA induced *PGM1/PGM2* promotion and *GFPT1/GFPT2* suppression in cells.
- Sugar metabolisms in HepG2 cells were more sensitive to TBBPS and TCBPA than TBBPA.

GRAPHICAL ABSTRACT

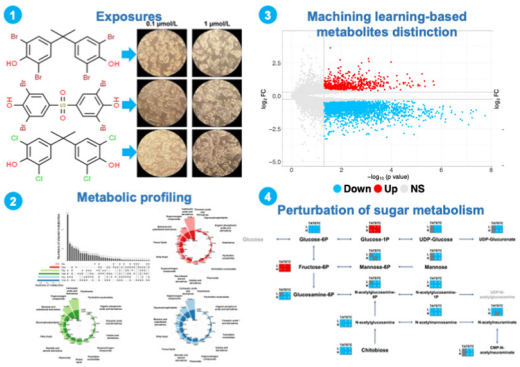

ARTICLE INFO

Editor: Daqiang Yin

Keywords:
Tetrabromobisphenol A
Brominated flame retardants
Metabolomics
Obesogens
Sugar metabolism

ABSTRACT

To date, increasing numbers of studies have shown the obesogenic effects of tetrabromobisphenol A (TBBPA). Tetrabromobisphenol S (TBBPS) and tetrachlorobisphenol A (TCBPA) are two common alternatives to TBBPA, and their environmental distributions are frequently reported. However, their toxicity and the associated potential health risks are poorly documented. Herein, we performed untargeted metabolomics to study the metabolic perturbations in HepG2 cells exposed to TBBPA and its alternatives. Consequently, no loss of cellular viability was observed in HepG2 cells exposed to 0.1 μmol/L and 1 μmol/L TBBPA, TBBPS and TCBPA. However, multivariate analysis and metabolic profiles revealed significant perturbations in glycerophospholipid and fatty acyl levels in HepG2 cells exposure to TBBPS and TCBPA. The evident increases in the glucose 1-phosphate and fructose 6-phosphate levels in HepG2 cells were proposed to be induced by the promotion of *PGM1/PGM2* and *GPI* gene expression and the suppression of *UPG2* and *GFPT1/GFPT2* gene expression. Our results suggest that TBBPS and TCBPA are more likely to disrupt liver metabolic homeostasis and potentially drive liver dysfunction than TBBPA. Our study is significant for the re-evaluation of the health risks associated with TBBPA and its alternatives TBBPS and TCBPA.

1. Introductions

Tetrabromobisphenol a (TBBPA) is one of the brominated flame retardants that is most extensively used in electronic devices and apparatuses (Liu et al., 2016). With an annual production of over 2 million tons (Yu et al., 2019), TBBPA is now ubiquitous in the environmental matrix and even detected in the breast milk of pregnant women (Covaci et al., 2009; Huang et al., 2014, 2020; Lankova et al., 2013; Li et al., 2021; Zhu et al., 2020). In the past decade, the potential toxicological effects of TBBPA have been widely reported (Dunnick et al., 2017; Nakajima et al., 2009; Parsons et al., 2019; Zhu et al., 2018). To date, increasing numbers of

* Corresponding authors.
E-mail addresses: yuyunjiang@scies.org (Y. Yu), lizhenchi@scies.org (Z. Li).

http://dx.doi.org/10.1016/j.scitotenv.2022.154847
Received 30 January 2022; Received in revised form 22 March 2022; Accepted 23 March 2022
Available online 28 March 2022

studies have pointed out the obesogenic effects of TBBPA. Early studies have reported increases in liver weight and serum cholesterol contents in rats orally administered TBBPA for one month (Choi et al., 2011; Tada et al., 2006), although the exposure dose (500 mg/kg) used in this study was irrelevant to that found in the real environment. In studies of the intrinsic mechanisms of the obesogenic effects of TBBPA, inconsistent findings have been reported. Studies on mouse 3T3-L1 cells revealed the role of TBBPA as a ligand that bound to peroxisome proliferator-activated receptor gamma (PPARγ), which induced fat accumulation in cells (Riu et al., 2011). TBBPA also triggered the early expression of genes in the glucocorticoid receptor (GR) signaling pathway and promoted early adipogenesis and lipogenesis in 3T3-L1 cells (Chappell et al., 2018). Moreover, a recent study suggested that TBBPA induced microRNA-103 expression and promoted adipogenesis (Woeller et al., 2017). Tetrabromobisphenol S (TBBPS) and tetrachlorobisphenol A (TCBPA) are two common alternatives to TBBPA that share similar chemical structures with TBBPA (Covaci et al., 2009; Qu et al., 2016). Currently, studies have shown the environmental distributions of TBBPS and TCBPA (Chu et al., 2005; Yang et al., 2014). In contrast to those of TBBPA, studies on the toxicological effects of TBBPS and TCBPA were fewer in number. Nevertheless, a previous study suggested that TCBPA could also be a ligand of the PPARγ signaling pathway (Riu et al., 2011), whereas TBBPS could affect hepatic differentiation (Yang et al., 2021). Although these studies revealed potential hepatic and obesogenic effects of TCBPA and TBBPS, the detailed mechanisms have not yet been elucidated. With regard to the potential obesogenic risks of TBBPA and its alternatives TBBPS and TCBPA, global profiling of the biological responses to these pollutants is urgent to explore the intrinsic mechanisms by which they execute obesogenic effects and will help in re-evaluating their associated health risks.

The liver is one of the most important organs for maintaining metabolic homeostasis in the human body (van den Berghe, 1991). Numerous studies have addressed the hepatic effects of TBBPA and some of its alternatives or derivatives. A previous transcriptome study found that 159 transcripts corresponding to 132 genes were differentially expressed in the livers of Wistar Han rats exposed to TBBPA (Dunnick et al., 2017). In addition, TBBPA and TCBPA prompted lipid deposition in HepG2 cells (Q. Liu et al., 2020). Moreover, the most recent study reported that an environmentally relevant dose of TBBPA (57 nmol/kg) altered the triacylglycerol and free fatty acid levels in mouse livers, which resulted in transcriptome perturbation (Qu et al., 2021). Therefore, TBBPA and its structurally similar alternatives may disrupt liver metabolic homeostasis and induce subsequent obesogenic effects.

To date, omics techniques have been applied to survey the global responses of study subjects exposed to environmental pollutants (Koh and Hwang, 2019); of these techniques, metabolomic profiling reveals imperceptible alterations of small molecules at metabolic levels and describes the true status of study subjects after exposure. In this study, untargeted metabolomics was performed to investigate the metabolic responses of HepG2 human hepatoma cells exposed to TBBPA and its alternatives TBBPS and TCBPA. We aim to demonstrate the perturbations of liver metabolic homeostasis after treatment with these pollutants and to explore the intrinsic mechanism of their obesogenic effects.

2. Material and methods

2.1. Chemicals

TBBPA (97%, Sigma-Aldrich, USA), TBBPS (98%, AccuStandard, USA), and TCBPA (98%, Sigma-Aldrich, USA) were dissolved in cell culture-grade dimethyl sulfoxide (DMSO) (Sigma-Aldrich, USA). LC-MS grade chemical methanol (Fisher, USA), acetonitrile (Merck, USA), water (Merck, USA), ammonium acetate (Sigma-Aldrich, USA) and ammonium hydroxide (Fisher, USA) were used to prepare the mobile phase.

2.2. Exposure and cell viability test

Considering that the reported concentration of TBBPA, TBBPS and TCBPA in human serum samples and in the environment (Fujii et al., 2014; Kim and Oh, 2014; Li et al., 2020; Yin et al., 2011), HepG2 cells were exposed to environmental relevant dose of TBBPA, TBBPS and TCBPA at 0.1 and 1.0 μmol/L in this study. HepG2 cells (ATCC HB-8065, USA) were cultured to perform cellular treatment experiments. The details of culture conditions, methods of exposures and cell viability tests (MTS method) are described in the supplementary file.

2.3. Metabolomic sample preparation

After 24 h of exposure, HepG2 cells were collected (cell density of 10^7 cells/mL), and mixture of chilled methanol, acetonitrile and water (*v*/v/v = 2:2:1) was added. The collected cells were immediately immersed in liquid nitrogen for 15 s and stored at −80 °C until the next process. Metabolite extraction and QC sample preparation processes were performed according to previous studies with some modifications (Tian et al., 2021b). The details are shown in the supplementary file.

2.4. Instrumental analysis

2.4.1. LC-QTOF-MS

Metabolites in the samples and the QC samples were analyzed by UHPLC (1290 Infinity LC Agilent Technologies, USA) coupled with quadrupole time-of-flight (QTOF) (AB Sciex TripleTOF 6600, USA). The mobile phase conditions, chromatographic programming, electrospray ionization settings and mass spectrometric parameters are described in the supplementary file.

2.4.2. qPCR

The primers were designed by Primer Blast online tools (https://www.ncbi.nlm.nih.gov/tools/primer-blast/). Total RNA was extracted from HepG2 cells by TRIzol reagent (Invitrogen, USA). Reverse transcription was performed by GoScript™ Reverse Transcription Mix Oligo (dT) (Promega, USA). The qPCR programming was set as follows: 95 °C for 10 min; stage 2: 95 °C for 15 s, 60 °C for 1 min; and 40 cycles. The selected primers used in this study are shown in Table S1 in the supplementary file.

2.5. Data processing and statistical analysis

2.5.1. Raw data processing

Raw data from LC-QTOF were converted into adaptable format, imported into R (v. 4.03) and processed by *XCMS* package (v. 3.14.1) for peak extraction, peak alignment, and retention time correction (Smith et al., 2006). In the generated raw feature table, the relative standard deviation (RSD) of features in QC samples was calculated, where the features with RSD > 20% were removed.

2.5.2. Metabolites identification

Human Metabolome Database (HMDB) metabolite data (https://hmdb.ca/downloads) were downloaded as a reference database. In the reference database, 114,222 metabolites annotated with 26 superclass, 328 class and 528 subclass were stored, 5658 of which were mutually stored in KEGG database. The precursor ion (MS1) of features in this study was browsed to the reference databases by a self-developed R script. The mass error threshold was set as 10 ppm. The product ion (MS2) spectra of the features were extracted and compared with the reference spectra in HMDB online databases (Wishart et al., 2018), and the commercial local database of Shanghai Applied Protein Technology Co., Ltd. The chemical taxonomy of metabolites was referenced to the superclass, class and subclass of metabolites in HMDB.

2.5.3. Multivariate data analysis

Partial least square discriminate analysis (PLS-DA) was performed by the *ropls* R package to determine the significantly changed metabolites (Thévenot et al., 2015). A permutation test (200 permutations) was used to evaluate the robustness of the model. The variable importance in the projection (VIP) value of each feature was calculated. VIP value > 1, Welch's *t*-test *p*-value < 0.05, and FC > 1.20 or FC < 0.83 were used to screen the significantly changed features.

2.5.4. Pathway analysis

Metabolite set enrichment analysis in MetaboAnalyst 5.0 online tools (https://www.metaboanalyst.ca/MetaboAnalyst/home.xhtml) was used for the pathway analysis, with significantly changed metabolites were used as the input (Chong et al., 2019; Pang et al., 2021). To cover more potential metabolic pathways affected by TBBPA and its alternatives, both KEGG and the Small Molecule Pathway Database (SMPDB) were selected as sources of the metabolic pathways, and the pathway analyses were performed separately (Frolkis et al., 2009; Jewison et al., 2014). The expected ratio and the FDR *p*-value of the resulting metabolic pathways were combined to evaluate the significance of their enrichment.

3. Results

3.1. Viability of HepG2 cells

When the exposure time was 24 h, no significant loss of cell viability was observed in the TBBPA, TBBPS and TCBPA groups at concentrations of 10, 20 and 20 μmol/L (Fig. 1a). In contrast, after 48 h of exposure, the viability of HepG2 cells exposed to TBBPA, TBBPS and TCBPA at doses of 2, 20 and 20 μmol/L was significantly decreased (p-value < 0.05) (Fig. 1a). A lower dose (0.1 μmol/L) and a higher exposure dose (1 μmol/L) were selected to perform the rest of the experiments. At both doses, no obvious morphological changes were found in HepG2 cells (Fig. 1b).

3.2. Metabolomic data

In the raw feature table, 12,548 (+) and 7070 (−) features were obtained, whereas 11,415 (+) and 6341 (−) features were retained in the clean feature table (RSD < 20%). Principal coordinate analysis (PCA) computed from both feature tables showed tightly clustering of QC samples (Fig. S1 a–d).

In all the samples, 2623 unique metabolites were identified and 159 unique chemical taxonomies were annotated. Carboxylic acids and derivatives, together with organooxygen compounds, were the two most annotated chemical taxonomies, accounting for 17.88% and 9.04%, respectively (Fig. S2). Next, several lipids were identified, such as fatty acyls (7.17%), glycerophospholipids (6.94%), prenol lipids (6.14%), steroids and steroid derivatives (4.54%).

3.3. Significantly changed metabolites

PLS-DA score plots showed that samples from the TBBPA-, TBBPS- and TCBPA-treated groups were well separated with those from the control group (Fig. S3 a–b). Permutation test results (200 iterations) validate the robust of the PLS-DA model (Fig. S4 a–b). VIP values were generated and were combined with volcano plots to screen the significantly changed features (Fig. S5 a–b). Consequently, the numbers of significantly changed features in the TAL-, TAH-, TSL-, TSH-, TCL- and TCH-treated groups compared with the control group were 474, 1605, 2788, 3442, 3050 and 3075 in the positive mode, whereas the numbers were 364, 900, 1422, 1811, 1785 and 1762 in the negative mode. Among them, the numbers of unique identified metabolites were 129, 313, 604, 670, 699 and 719 in the TAL, TAH, TSL, TSH, TCL and TCH groups, respectively, whereas the numbers of metabolites exclusively found in these groups were 29, 65, 28, 58, 90 and 67, respectively (Fig. 2a). The TSL, TSH, TCL and TCH groups shared the highest numbers of common metabolites (242). The most annotated chemical taxonomies of the significantly changed metabolites are shown in Fig. 2b–d. Carboxylic acids and derivatives, and organooxygen compounds were the two most annotated chemical taxonomies of all the

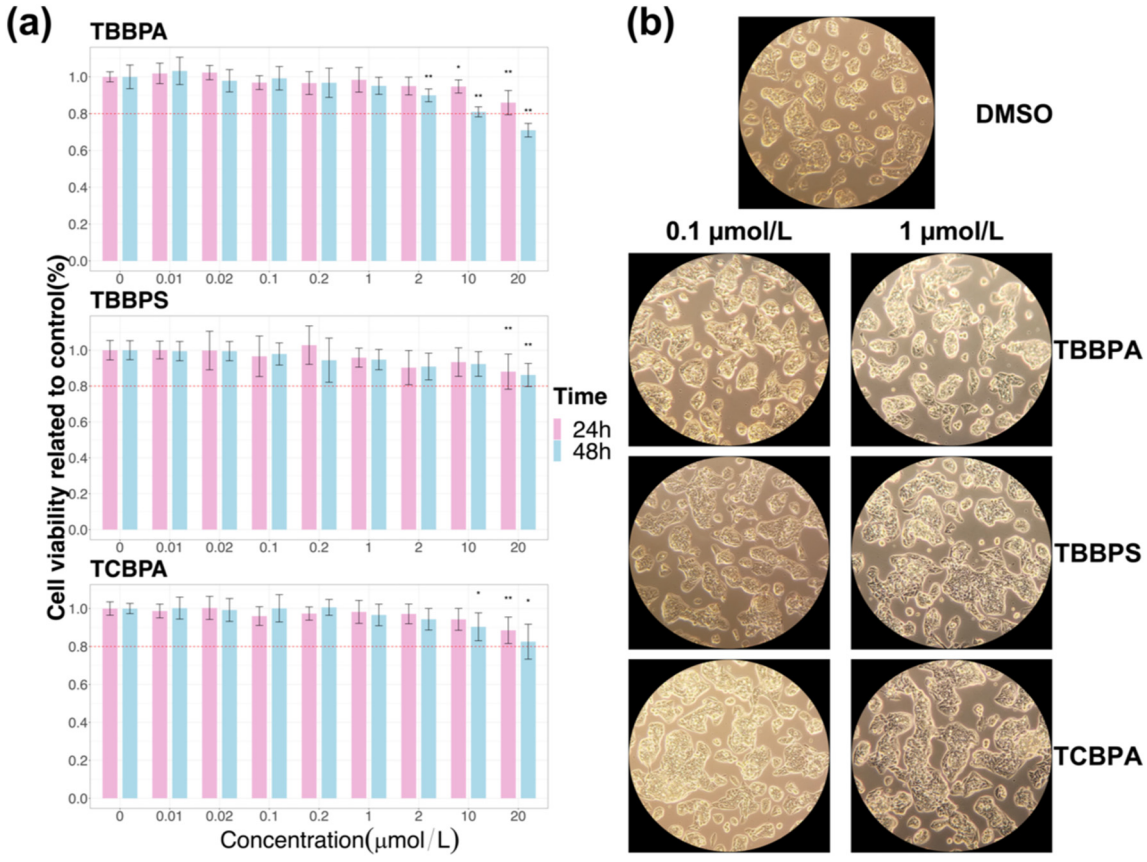

Fig. 1. HepG2 cells viability and morphology. (a) Error bar charts showing relative cell viability of HepG2 exposed to TBBPA, TBBPS and TCBPA (*Wilcoxon test p-value < 0.05, **p-value < 0.01). Red horizontal dashed lines stand for the 80% of the related cell viability. (b) Cells morphology images of HepG2 exposed to TBBPA, TBBPS and TCBPA at 0.1 μmol/L and 1 μmol/L for 24 h.

significantly changed metabolites. In the following, lipids such as fatty acyls, prenol lipids, steroids and steroid derivatives, and glycerophospholipids were predominantly annotated. The percentages of significantly changed metabolites identified as fatty acyls were generally higher in the 1 μmol/L group than in the 0.1 μmol/L. Similarly, the percentages of steroids and steroid derivatives were also higher in the 1 μmol/L group. The number of metabolites identified as glycerophospholipids was found to be much higher in the TBBPS- and TCBPA-treated groups than in the TBBPA-treated groups.

3.4. Changing profiles of metabolites annotated with glycerophospholipids and fatty acyls

In the TBBPA-treated groups, no significant clustered pattern could be observed in metabolites annotated with glycerophospholipids (Fig. 3a). In contrast, a portion of metabolites in the TBBPS- and TCBPA-treated groups were found to be significantly reduced compared with that in the control group, and these metabolites included glycerophosphocholine, glycerol 2-phosphate (P), and glycerol-3P (Fig. 3a). Another portion of glycerophospholipids in the TBBPS-treated groups was significantly increased compared to that in the control group; however, most of these molecules changed in a dose-dependent manner in the TCBPA-treated groups, including some phosphocholine (Pc) and phosphoethanolamine (Pe) derivatives such as Pc 40:7, Pc 38:7 and Pe 38:7. The majority of metabolites annotated with fatty acyls were found to be significantly decreased in the TBBPS- and TCBPA-treated groups compared with the control group, while only a few of them showed the opposite trend (Fig. 3b).

3.5. Significantly enriched metabolic pathways

The most significantly enriched metabolic pathways identified from KEGG included purine metabolism, amino/nucleotide sugar metabolism, pyrimidine metabolism, and glycerophospholipid metabolism, whereas for SMPDB, pyrimidine metabolism, glutamate metabolism, purine metabolism, and amino/nucleotide sugar metabolism were the most significantly enriched (Fig. 4a–b). Accordingly, amino/nucleotide sugar metabolism and glycerophospholipid metabolism were selected as metabolic pathways of interest to study the potential obesogenic effects of TBBPA and its alternatives. All the identified metabolites in these two pathways were extracted (Table 1). In amino/nucleotide sugar metabolism, glucose-1P and fructose-6P increased in almost all the samples of the TBBPA-, TBBPS- and TCBPA-treated groups compared with the control (Fig. 4c). In contrast, mannose-6P, *N*-acetylneuraminate, glucosamine-6P, glucose-6P and uridine diphosphate (UDP)-glucuronate diminished in the TBBPS- and TCBPA-treated groups. On the other hand, in glycerophospholipid metabolism, elevations in phosphorylcholine and ethanolamine in the TBBPS- and TCBPA-treated groups were observed (Fig. 4d), while most of the rest of the metabolites, including cytidine diphosphate (CDP)-choline and glycerol-3P, reduced

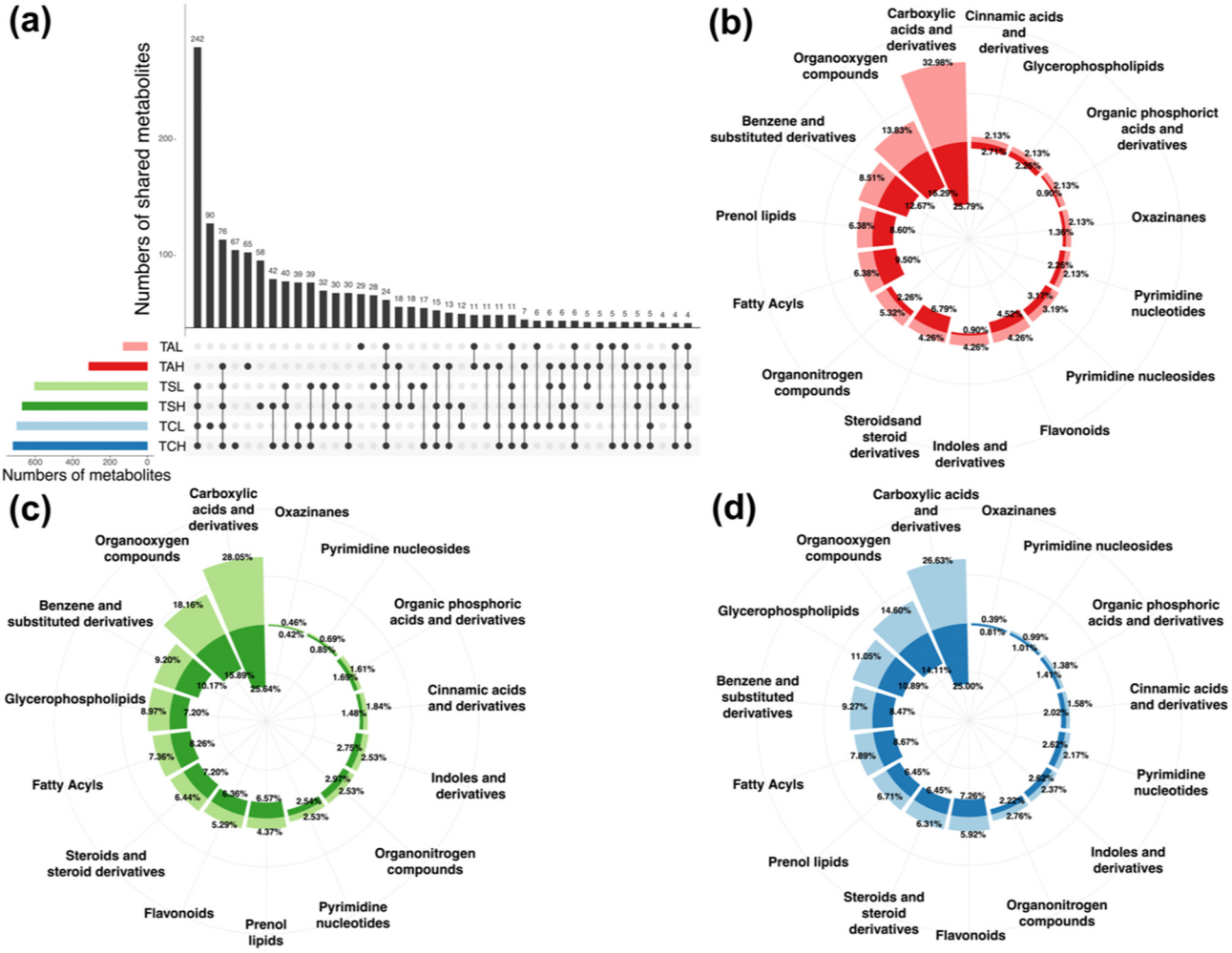

Fig. 2. Significantly changed metabolites and their chemical taxonomies. (a) Venn plot showing the mutually found metabolites in different exposure groups. Bars on the left: total amounts of identified and significantly changed metabolites; bars on the top: the numbers of mutually or exclusive found metabolites in selected groups. Percentage bar chars of the most annotated chemical taxonomies in the exposure groups of (b) TBBPA, (c) TBBPS and (d) TCBPA. Bars on the outer/inner circles represent groups of exposure doses of 0.1/1 μmol/L.

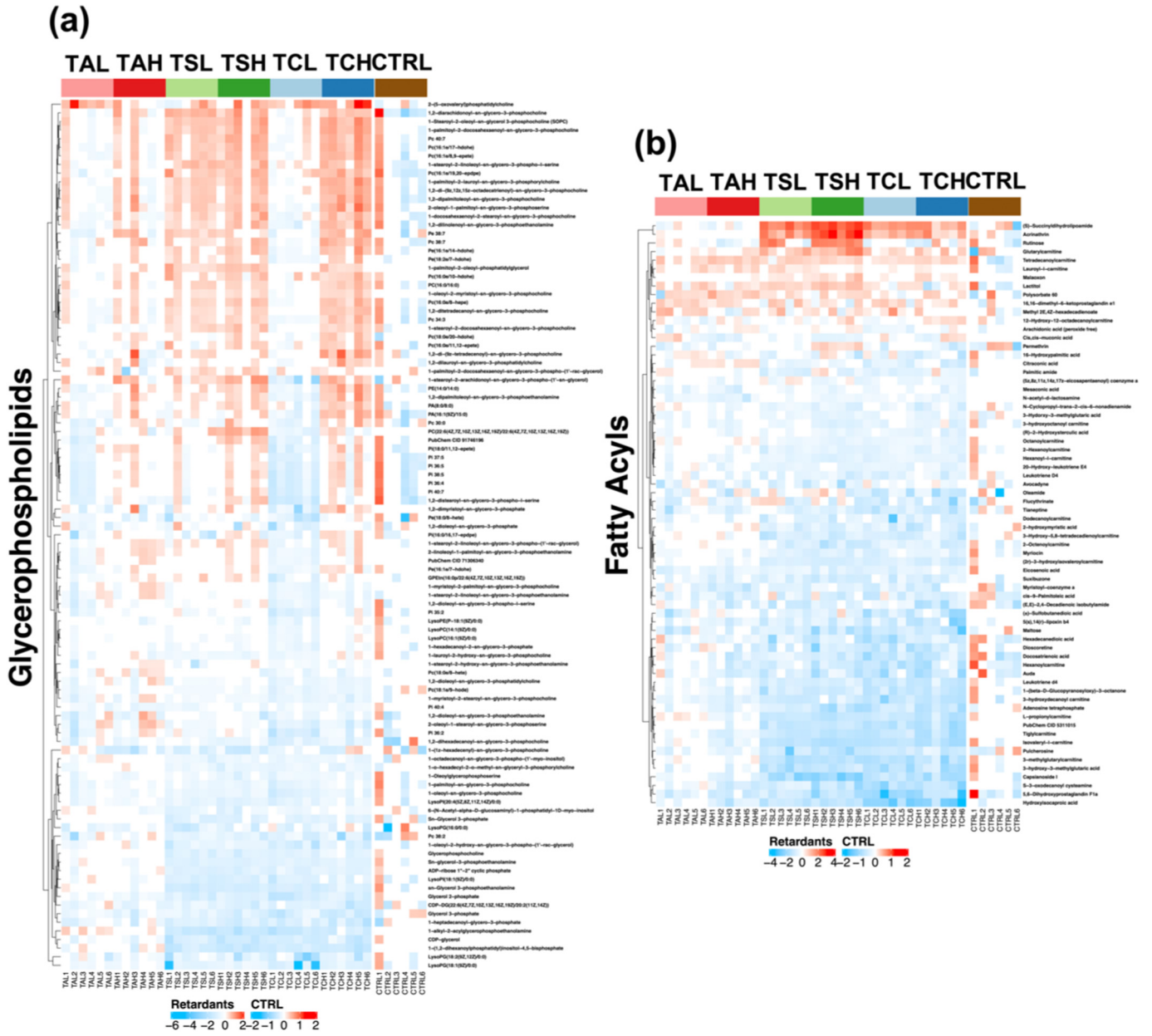

Fig. 3. Glycerophospholipids and fatty aclys changing profiles. Heatmaps showing significantly changed metabolites in HepG2 cells annotated with (a) glycerophospholipids and (b) fatty aclys.

significantly. To inspect the metabolic keynotes in these two pathways, the identified metabolites and their average FC related to the control are shown in Fig. 4e–f.

To further validate the activation of amino/nucleotide sugar metabolism and glycerophospholipid metabolism, the genes involved and their relative expression levels were measured (Fig. 5). Notably, *PGM1* expression was significantly regulated by both 0.1 μmol/L and 1 μmol/L TBBPS and TCBPA as well as 1 μmol/L TBBPA. However, dose-dependent effects could be found in the TBBPS- and TCBPA-treated groups, in which *UGP2* expression was only significantly affected by the higher doses (1 μmol/L). Both 0.1 and 1 μmol/L TBBPS and the high dose of TBBPA significantly raised the relative expression of *GPI*, while the expressions of *GFPT1* and *GFPT2* changed in opposite trend in TBBPS- and TCBPA-treated groups. The relative expression of *MPI* and genes encoding hexokinase (*HK1*, *HK2* and *HKDC1*) were found significantly upregulated in multiple groups (Fig. 5). Besides, the significant upregulation of *CHKB* was only observed in TBBPS-treated groups, whereas the downregulation of *PCYT1A*/*PCYT1B* were found in all the groups. Interestingly, *GPCPD1* expression significant down-regulated only in the groups of 1 μmol/L.

4. Discussion

4.1. TBBPS and TCBPA affect liver sugar metabolism

Previous studies have shown the obesogenic effects of environmental pollutants (Gupta et al., 2020). Considering that TBBPA has been reported to be an inducer of adipogenesis (Akiyama et al., 2015; Q.S. Liu et al., 2020), studies of the obesogenic effects of its structurally similar alternatives TBBPS and TCBPA are a high priority. In the present study, one of the most affected modules in amino/nucleotide sugar metabolism includes the reactions that transform glucose to UDP-glucose. The significant perturbations of the metabolites involved in this module implied the disruption of glucose metabolism in liver cells exposed to TBBPA and its alternatives. Other brominated flame retardants, such as brominated diphenyl ether

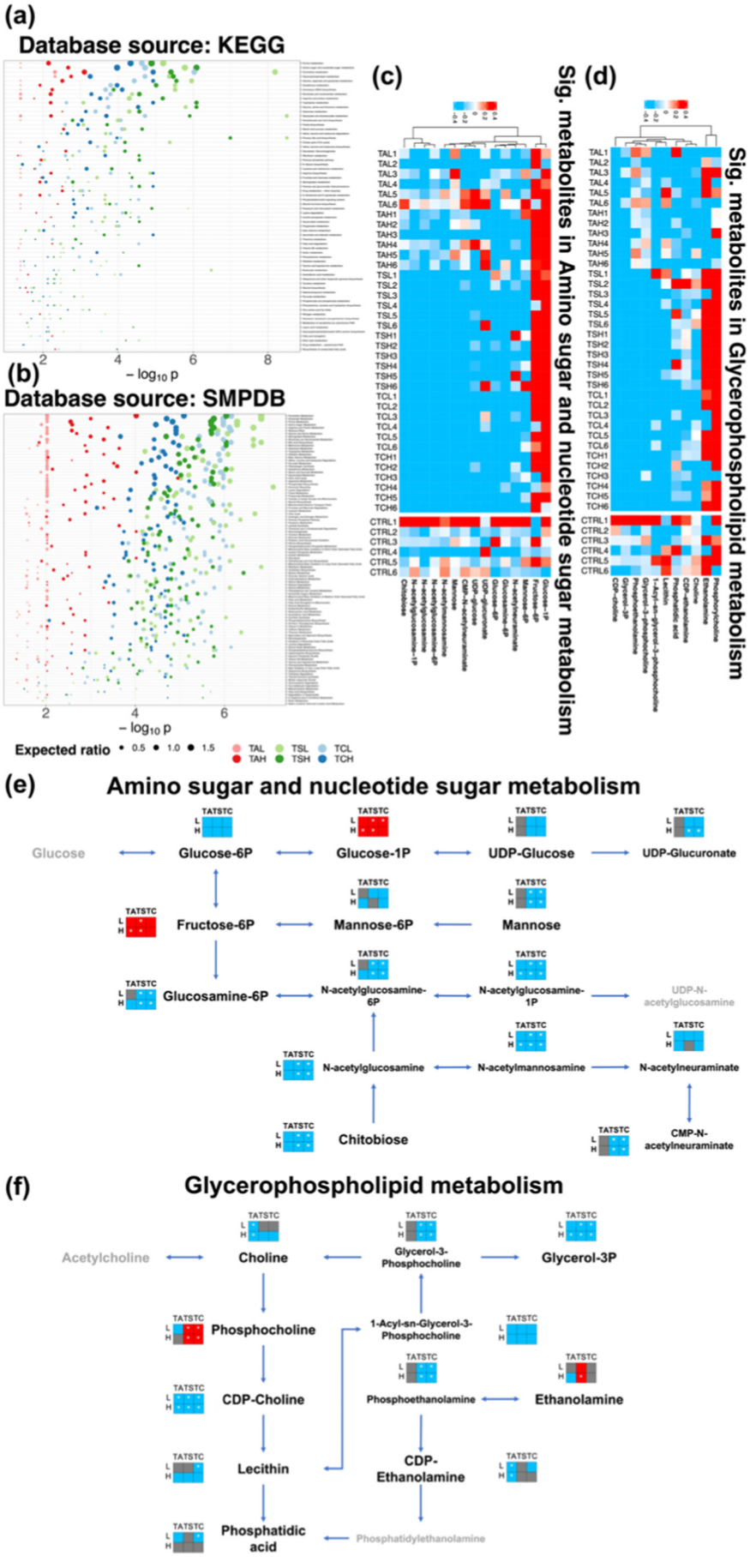
(a)
Database source: KEGG
– log10 p
(b)
Database source: SMPDB
– log10 p
Expected ratio
TAL
TAH
TSL
TSH
TCL
TCH
(c)
Sig. metabolites in Amino sugar and nucleotide sugar metabolism
(d)
Sig. metabolites in Glycerophospholipid metabolism
(e)
Amino sugar and nucleotide sugar metabolism
Glucose
Glucose-6P
Glucose-1P
UDP-Glucose
UDP-Glucuronate
Fructose-6P
Mannose-6P
Mannose
Glucosamine-6P
N-acetylglucosamine-6P
N-acetylglucosamine-1P
UDP-N-acetylglucosamine
N-acetylglucosamine
N-acetylmannosamine
N-acetylneuraminate
Chitobiose
CMP-N-acetylneuraminate
(f)
Glycerophospholipid metabolism
Acetylcholine
Choline
Glycerol-3-Phosphocholine
Glycerol-3P
Phosphocholine
1-Acyl-sn-Glycerol-3-Phosphocholine
CDP-Choline
Phosphoethanolamine
Ethanolamine
Lecithin
CDP-Ethanolamine
Phosphatidic acid
Phosphatidylethanolamine

Table 1
Significantly changed metabolites in the amino/nucleotide sugar metabolism and glycerophospholipid metabolism.

Metabolites	*m/z* (Da)	Adduct	Database ID	Adduct *m/z* (Da)	Mass error (ppm)	Pathways
Chitobiose	407.16463	$[M + H\text{-}H_2O]^+$	C01674	407.1666	4.84	Amino sugar and nucleotide sugar metabolism
CMP-*N*-acetylneuraminate	613.13654	$[M\text{-}H]^-$	C00128	613.1400	5.64	
Fructose-6P	259.02208	$[M\text{-}H]^-$	C05345	259.0224	1.24	
Glucosamine-6P	260.05188	$[M + H]^+$	C00352	260.0530	4.31	
Glucose-1P	241.01048	$[M\text{-}H\text{-}H_2O]^-$	C00103	241.0113	3.40	
Glucose-6P	519.04850	$[2\ M\text{-}H]^-$	C00092	519.0522	7.13	
Mannose-6P	243.02553	$[M + H\text{-}H_2O]^+$	C00275	243.0270	6.05	
Mannose	179.05558	$[M\text{-}H]^-$	C00936	179.0561	2.90	
N-acetylglucosamine	204.08620	$[M + H\text{-}H_2O]^+$	C00140	204.0872	4.90	
N-acetylglucosamine-1P	300.04751	$[M\text{-}H]^-$	C04256	300.0490	4.97	
N-acetylglucosamine-6P	284.05210	$[M + H\text{-}H_2O]^+$	C00357	284.0536	5.28	
N-acetylmannosamine	220.08173	$[M\text{-}H]^-$	C00645	220.0827	4.41	
N-acetylneuraminate	308.09661	$[M\text{-}H]^-$	C00270	308.0987	6.78	
UDP-glucose	565.04577	$[M\text{-}H]^-$	C00029	565.0477	3.42	
UDP-glucuronate	598.06500	$[M + NH_4]^+$	C00167	598.0681	5.18	
1-Acyl-sn-Glycerol-3-Phosphocholine	540.30920	$[M\text{-}H]^-$	C04230	540.3096	0.74	Glycerophospholipid metabolism
CDP-choline	489.11209	$[M + H]^+$	C00307	489.1146	5.13	
CDP-ethanolamine	445.04960	$[M\text{-}H]^-$	C00570	445.0531	7.86	
Choline	104.10662	M^+	C00114	104.1075	8.45	
Ethanolamine	103.08581	$[M + ACN + H]^+$	C00189	103.0866	7.66	
Glycerol-3P	173.01973	$[M + H]^+$	C00093	173.0210	7.34	
Glycerol-3-Phosphocholine	258.11010	$[M + H]^+$	C00670	258.1101	0.00	
Lecithin	756.54614	$[M + Na]^+$	C00157	756.5514	6.95	
Phosphatidic acid	417.23849	$[M\text{-}H\text{-}H_2O]^-$	HMDB0007851	417.2406	5.06	
Phosphocholine	184.07314	M^+	C00588	184.0739	4.13	
Phosphoethanolamine	140.01124	$[M\text{-}H]^-$	C00346	140.0118	4.00	

(BDE)-47 and BDE-28, have also been proposed to cause or correlate with disordered glucose metabolism (Kamstra et al., 2014; Vuong et al., 2021). Moreover, a recent metabolomics study demonstrated that bisphenol A (BPA), which is the debrominated form of TBBPA, altered glucose metabolism and blocked the TCA cycle in mouse livers (Ji et al., 2020). Therefore, it is estimated either the bisphenol groups or the brominated groups of TBBPA and its alternatives TBBPS and TCBPA exerted effects on liver glucose metabolism.

The increase of glucose-1P and opposite findings found between the relative expression of *PGM1/PGM2* (upregulated) and *UGP2* (downregulated) suggested that the expression of the upstream phosphoglucomutase was promoted while the expression of the downstream UDP-glucose pyrophosphorylase was inhibited in HepG2 cells, which caused the elevations of glucose-1P. Glucose-1P is an important participant in glucose metabolism and glycolysis, which are associated with glycerate and pyruvate metabolism and may further affect the tricarboxylic acid (TCA) cycle and fatty acid metabolism (Han et al., 2016). In the pathway analysis, the TCA cycle in HepG2 cells was found to be significantly enriched, especially in the TBBPS and TCBPA groups (Fig. 4a–b), which suggested that TBBPS and TCBPA were more likely to affect glucose-1P metabolism and the subsequent TCA cycle to further cause hepatic metabolic disorder.

Another module in this pathway is UDP-*N*-acetylglucosamine biosynthesis, which includes the reactions that transform glucose to UDP-*N*-acetylglucosamine. In this module, the elevation of fructose-6P was suggested by the promotion of glucose-6P isomerase and the inhibition of glutamine-fructose-6P transaminase, which further affected the downstream UDP-*N*-acetylglucosamine metabolism. UDP-*N*-acetylglucosamine was recently proposed to be a potential biomarker of glucolipotoxicity (Yousf et al., 2019), which suggested that the perturbations of its metabolism through TBBPA, TBBPS and TCBPA in this study were likely to induce glucose and lipid metabolic disorders. In addition, fructose-6P is a key intermediate in fructose and mannose metabolism in the liver. Mannose involved in the metabolism was significantly reduced in the TBBPS- and TCBPA-treated groups at both doses in this study. Recent studies revealed that mannose supplementation was crucial for altering the mouse gut microbiome and preventing harmful effects from high-fat diets (Sharma et al., 2018). Moreover, mannose metabolism was closely correlated with human hepatic stellate cell activation and hepatic fibrosis (DeRossi et al., 2019). Accordingly, TBBPS- and TCBPA-induced mannose reductions might trigger liver dysfunction or obesity. In both modules of amino/nucleotide sugar metabolism, the number of significantly changed genes and metabolites in the TBBPA-treated groups was comparatively less than that in the TBBPS- or TCBPA-treated groups, which suggested that this pathway was more sensitive to TBBPS and TCBPA.

4.2. Metabolic perturbations in glycerophospholipid metabolism

Glycerophospholipids are small molecules whose perturbations are frequently reported in diseased liver (Gorden et al., 2011; Kartsoli et al., 2020; Wang et al., 2016). Interchanged with acetylcholine by acetylcholinesterase and choline acetylase, the upstream choline in the pathway was found to be significantly reduced in TBBPA-treated HepG2 cells. A recent study suggested that obesity-induced fatty liver affected choline transportation through the inhibition of choline transporters (O'Dwyer et al., 2020), which suggested that the significant reduction in choline in HepG2 cells through TBBPA exposure in this study could eventually lead to fatty liver. Currently, the number of studies connecting choline contents in the liver and exposure to TBBPA or its alternatives is very limited. Nevertheless, metabolic profiling showed that administration of polybrominated diphenyl ethers could reduce rat urine choline levels (Jung et al., 2017). Moreover, another metabolomics study on BPA exposure revealed the perturbation of choline metabolism (Chen et al., 2014). Therefore, choline reduction in the liver in this study may be due to the brominated or bisphenol groups of TBBPA. On the other hand, the results of qPCR in this study suggested the promotion of choline acetylase phosphate and the inhibition of cytidylyltransferase, which blocked the transformation from phosphocholine to CDP-choline.

Fig. 4. Pathway analysis of HepG2 cells exposed to TBBPA, TBBPS and TCBPA. Scatter plots of metabolite set enrichment analysis results implemented with database sources of (a) KEGG and (b) SMPDB. Heatmaps showing changing profiles of metabolites in pathways of (c) amino/nucleotide sugar metabolism and (d) glycerophospholipid metabolism. (e)–(f) Metabolic flux in (e) amino/nucleotide sugar metabolism and (f) glycerophospholipid metabolism. Red (FC > 1.2), blue (FC < 0.83) and gray (0.83 ≤ FC ≤ 1.2) cells indicate the FC of the metabolites in TBBPA-, TBBPS- and TCBPA-treated groups compared to the control (*VIP > 1 & Welch's *t*-test *p*-value < 0.05).

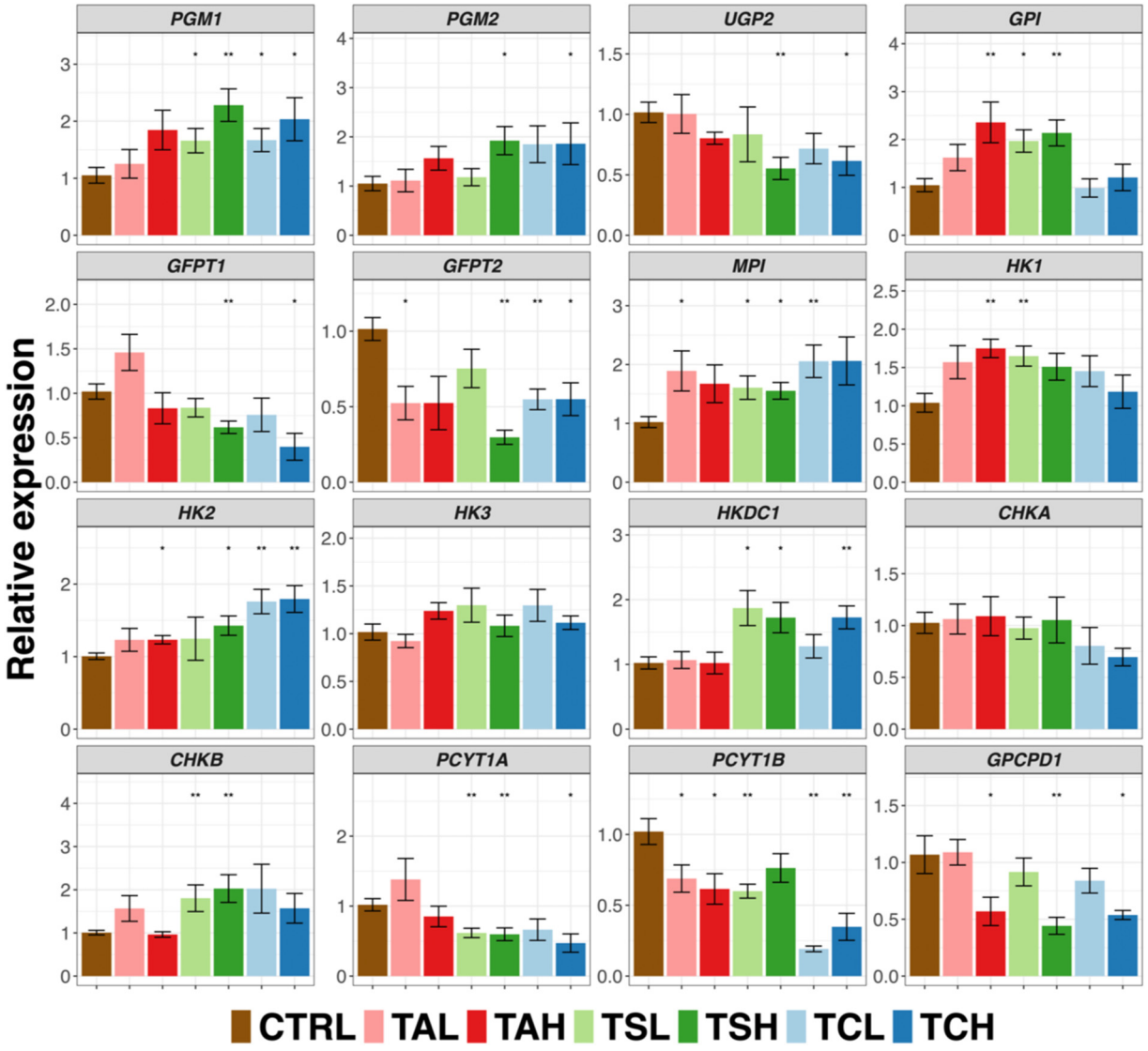

Fig. 5. Gene expression involved in pathways of amino/nucleotide sugar metabolism, and glycerophospholipid metabolism. Bar charts showing the relative expressions of the involved genes (*Wilcoxon rank sum test *p*-value < 0.05; ***p*-value < 0.01). *PGM1/PGM2*: phosphoglucomutase; *UGP2*: UDP-glucose pyrophosphorylase 2; *GPI*: glucose-6-phosphate isomerase; *GFPT1/GFPT2*: glutamine-fructose-6-phosphate transaminase; *MPI*: mannose phosphate isomerase; *HK1/HK2/HK3/HKDC1*: hexokinase; *CHKA/CHKB*: choline kinase; *PCYT1A/PCYT1B*: phosphate cytidylyltransferase; *GPCPD1*: glycerophosphocholine phosphodiesterase.

Metabolomics study revealed that phosphocholine was one of the main metabolites altered in ethanol-treated livers (Wang et al., 2015). Therefore, TBBPS- and TCBPA-induced elevations in phosphocholine in this study suggested potential impairments to the liver. Results in this study also suggested that glycerol-3-phosphocholine metabolism in HepG2 cells was affected by TBBPA, TBBPS and TCBPA and led to abnormal glycerol-3P contents in HepG2 cells. Glycerol-3P is a metabolic keystone in several metabolic pathways, such as glycolysis, glycerolipid and free fatty acid cycle, gluconeogenesis, and energy metabolism (Possik et al., 2021), and is associated with liver dysregulations, injuries and obesity (Hakim et al., 2021; Hammond et al., 2002). Therefore, perturbation of glycerol-3P by TBBPA and its alternatives TBBPS and TCBPA could adversely affect liver metabolic homeostasis and induce further liver dysfunction or obesity.

Apart from amino/nucleotide sugar metabolism and glycerophospholipids metabolism, some other metabolic pathways were significantly enriched in this study, such as purine metabolism, pyrimidine metabolism, and glutathione metabolism (Fig. 4a–b). Metabolomics study demonstrated that exposure of mixed pollutants including TBBPA significantly affected purine metabolism, pyrimidine and purine metabolisms, and glutathione metabolism in human breast cancer cells (M. Liu et al., 2020), which implied that these pathways were susceptible in cells exposed to various chemicals. In addition, these pathways were frequently reported in the studies of organic/inorganic pollutants exposures in different cell types and were related to the cell energy metabolism (Tian et al., 2021a, 2021b). In this study, TBBPA, TBBPS and TCBPA might interfere energy metabolism of HepG2 cells and induced further obesogenic effects. However, further study on the metabolic flux in these pathways is required to validate the energy metabolism status of HepG2 cells exposed to TBBPA, TBBPS and TCBPA.

4.3. Potential obesogenic effects produced by TBBPA, TBBPS and TCBPA

The toxicological effects of TBBPA and the potential health risk associated with TBBPA have been thoroughly reported. The most recent RNA-seq study of HepG2 cells with long-term exposure to TBBPA at low concentrations (1 nmol/L) revealed its potential to cause metabolic disorders through the Ras signaling pathway (Lu et al., 2021). For TBBPA alternatives such as TBBPS and TCBPA, transcriptomics studies have shown their disruptive effects on hepatic differentiation (Yang et al., 2021). However, in exposure studies of TBBPA and its alternatives, the cellular responses at

metabolic levels are poorly documented, which hinders the understanding of the intrinsic mechanism of their toxicological effects. In this study, both the cell viability tests and the cell morphology images showed no apparent effects on HepG2 cells exposed to TBBPA and its alternatives TBBPS and TCBPA at concentrations of 0.1 and 1 μmol/L. However, metabolic profiling characterized the differences. PCA is an unsupervised machine learning method that reveals data dissimilarity. The PCA score plots in this study suggested that the metabolic disturbance and cellular response in HepG2 cells were similar in the TBBPS- and TCBPA-treated groups and differed from those in the TBBPA-treated group (Fig. S1). The discernible differences in the changing profiles of glycerophospholipid and fatty acyls between the HepG2 cells in the TBBPA-treated groups and the TBBPS/TCBPA groups also showed their dissimilar effects on liver cells. A previous study showed that TCBPA was similar to TBBPA in activating the PPARγ signaling pathway, which suggests their similar obesogenic effects (Riu et al., 2011). However, a recent study contradicted the conclusion that TCBPA induced more lipid deposition in HepG2 cells than TBBPA (Q. Liu et al., 2020). On the other hand, TBBPS was reported to have weaker cytotoxic effects on blood mononuclear cells than TBBPA (Włuka et al., 2020; Yang et al., 2021). However, the most recent study showed that TBBPS exerted strong effects on circadian rhythm-related genes of zebrafish (Ding et al., 2022). In this study, we found that more genes and metabolites were significantly perturbed in pathways of amino/nucleotide sugar metabolism and glycerophospholipid metabolism in the TBBPS- and TCBPA-treated groups compared with those in the TBBPA-treated groups, which at least indicated that these metabolisms in liver were more susceptible to TBBPS and TCBPA than to TBBPA. Although metabolites and related genes were identified in amino/nucleotide sugar metabolism and glycerophospholipid metabolism in this study, further research on the activities of the enzymes involved in the pathways is required to confirm their perturbations. Besides, TBBPA, TBBPS and TCBPA are similar in chemical structure, however, are different in molecular descriptors. Currently, novel data mining approaches have been proposed that implemented artificial neural networks and molecular descriptor (Li et al., 2019), which could elucidate whether and how do the different molecular descriptors of TBBPA and its alternatives contribute to different obesogenic effects. In addition, animal studies or investigations of large sample batch cohorts are advised to validate and distinguish the hepatic and obesogenic effects of TBBPA, TBBPS and TCBPA.

5. Conclusion

In this study, metabolites in HepG2 cells exposed to TBBPA, TBBPS and TCBPA were profiled by untargeted metabolomics. At exposure doses of 0.1 μmol/L and 1 μmol/L, no significant difference was observed in cell viability and morphology. However, multivariate analysis, glycerophospholipid and fatty acyl changing profiles revealed that TBBPS and TCBPA induced apparent metabolic perturbation in HepG2 cells. The metabolite set enrichment analysis results revealed the significant enrichment of amino/nucleotide sugar and glycerophospholipid metabolism, in which the genes and metabolites were more affected in the TBBPS- and TCBPA-treated groups. The significant increases in glucose-1P and fructose-6P levels by TBBPS and TCBPA were caused by the promotion of upstream gene expression and the inhibition of downstream gene expression. Our results suggest that TBBPS and TCBPA are more likely to produce hepatic and obesogenic effects than TBBPA.

CRediT authorship contribution statement

Yunjiang Yu: Conceptualization, Methodology, Writing - Review & Editing, Funding acquisition. **Chaojie Hao**: Software, Formal analysis, Writing - Original draft preparation. **Mingdeng Xiang**: Writing - Original Draft, Investigation. **Jinglin Tian**: Visualization, Writing - Review & Editing. **Hongxuan Kuang**: Writing - Review & Editing. **Zhenchi Li**: Conceptualization, Methodology, Software, Validation, Formal analysis, Writing - Original Draft, Visualization, Writing - Review & Editing, Funding acquisition.

Declaration of competing interest

The authors declare that they have no known competing financial interests or personal relationships that could have appeared to influence the work reported in this paper.

Acknowledgement

This work was supported by the National Natural Science Foundation of China (Grant Nos. 41931298 and 21876059) and Basic Research Foundation of National Commonwealth Research Institute (No. PM-zx703-202104-049).

Appendix A. Supplementary data

Supplementary data to this article can be found online at https://doi.org/10.1016/j.scitotenv.2022.154847.

References

Akiyama, E., Kakutani, H., Nakao, T., Motomura, Y., Takano, Y., Sorakubo, R., Mizuno, A., Aozasa, O., Tachibana, K., Doi, T., Ohta, S., 2015. Facilitation of adipocyte differentiation of 3T3-L1 cells by debrominated tetrabromobisphenol A compounds detected in Japanese breast milk. Environ. Res. 140, 157–164. https://doi.org/10.1016/j.envres.2015.03.035.

Chappell, V.A., Janesick, A., Blumberg, B., Fenton, S.E., 2018. Tetrabromobisphenol-A promotes early adipogenesis and lipogenesis in 3T3-L1 cells. Toxicol. Sci. 166, 332–344. https://doi.org/10.1093/toxsci/kfy209.

Chen, M., Zhou, K., Chen, X., Qiao, S., Hu, Y., Xu, Bo, Xu, Bin, Han, X., Tang, R., Mao, Z., Dong, C., Wu, D., Wang, Y., Wang, S., Zhou, Z., Xia, Y., Wang, X., 2014. Metabolomic analysis reveals metabolic changes caused by bisphenol A in rats. Toxicol. Sci. 138, 256–267. https://doi.org/10.1093/toxsci/kfu016.

Choi, J.S., Lee, Y.J., Kim, T.H., Lim, H.J., Ahn, M.Y., Kwack, S.J., Kang, T.S., Park, K.L., Lee, J., Kim, N.D., Jeong, T.C., Kim, S.G., Jeong, H.G., Lee, B.M., Kim, H.S., 2011. Molecular mechanism of tetrabromobisphenol a (tbbpa)-induced target organ toxicity in Sprague-Dawley male rats. Toxicol. Res. 27, 61–70. https://doi.org/10.5487/TR.2011.27.2.061.

Chong, J., Wishart, D.S., Xia, J., 2019. Using MetaboAnalyst 4.0 for comprehensive and integrative metabolomics data analysis. Curr. Protoc. Bioinformatics 68, 1–128. https://doi.org/10.1002/cpbi.86.

Chu, S., Haffner, G.D., Letcher, R.J., 2005. Simultaneous determination of tetrabromobisphenol A, tetrachlorobisphenol A, bisphenol A and other halogenated analogues in sediment and sludge by high performance liquid chromatography-electrospray tandem mass spectrometry. J. Chromatogr. A 1097, 25–32. https://doi.org/10.1016/j.chroma.2005.08.007.

Covaci, A., Voorspoels, S., Abdallah, M.A.E., Geens, T., Harrad, S., Law, R.J., 2009. Analytical and environmental aspects of the flame retardant tetrabromobisphenol-A and its derivatives. J. Chromatogr. A 1216, 346–363. https://doi.org/10.1016/j.chroma.2008.08.035.

DeRossi, C., Bambino, K., Morrison, J., Sakarin, I., Villacorta-Martin, C., Zhang, C., Ellis, J.L., Fiel, M.I., Ybanez, M., Lee, Y.A., Huang, K.lin, Yin, C., Sakaguchi, T.F., Friedman, S.L., Villanueva, A., Chu, J., 2019. Mannose phosphate isomerase and mannose regulate hepatic stellate cell activation and fibrosis in zebrafish and humans. Hepatology 70, 2107–2122. https://doi.org/10.1002/hep.30677.

Ding, Y., Dong, X., Feng, W., Mao, G., Chen, Y., Qiu, X., Chen, K., Xu, H., 2022. Tetrabromobisphenol S alters the circadian rhythm network in the early life stages of zebrafish. Sci. Total Environ. 806, 150543. https://doi.org/10.1016/j.scitotenv.2021.150543.

Dunnick, J.K., Morgan, D.L., Elmore, S.A., Gerrish, K., Pandiri, A., Ton, T.V., Shockley, K.R., Merrick, B.A., 2017. Tetrabromobisphenol A activates the hepatic interferon pathway in rats. Toxicol. Lett. 266, 32–41. https://doi.org/10.1016/j.toxlet.2016.11.019.

Frolkis, A., Knox, C., Lim, E., Jewison, T., Law, V., Hau, D.D., Liu, P., Gautam, B., Ly, S., Guo, A.C., Xia, J., Liang, Y., Shrivastava, S., Wishart, D.S., 2009. SMPDB: the small molecule pathway database. Nucleic Acids Res. 38, 480–487. https://doi.org/10.1093/nar/gkp1002.

Fujii, Y., Nishimura, E., Kato, Y., Harada, K.H., Koizumi, A., Haraguchi, K., 2014. Dietary exposure to phenolic and methoxylated organohalogen contaminants in relation to their concentrations in breast milk and serum in Japan. Environ. Int. 63, 19–25. https://doi.org/10.1016/j.envint.2013.10.016.

Gorden, D.L., Ivanova, P.T., Myers, D.S., McIntyre, J.O., VanSaun, M.N., Wright, J.K., Matrisian, L.M., Brown, H.A., 2011. Increased diacylglycerols characterize hepatic lipid changes in progression of human nonalcoholic fatty liver disease; comparison to a murine model. PLoS One 6, e22775. https://doi.org/10.1371/journal.pone.0022775.

Gupta, R., Kumar, P., Fahmi, N., Garg, B., Dutta, S., Sachar, S., Matharu, A.S., Vimaleswaran, K.S., 2020. Endocrine disruption and obesity: a current review on environmental obesogens. Curr. Res. Green Sustain. Chem. 3, 100009. https://doi.org/10.1016/j.crgsc.2020.06.002.

Hakim, A., Moll, M., Brancale, J., Liu, J., Lasky-Su, J.A., Silverman, E.K., Vilarinho, S., Jiang, Z.G., Pita-Juárez, Y.H., Vlachos, I.S., Zhang, X., Åberg, F., Afdhal, N.H., Hobbs, B.D., Cho, M.H., 2021. Genetic variation in the mitochondrial glycerol-3-phosphate acyltransferase is associated with liver injury. Hepatology, 0–2 https://doi.org/10.1002/hep.32038.

Hammond, L.E., Gallagher, P.A., Wang, S., Hiller, S., Kluckman, K.D., Posey-Marcos, E.L., Maeda, N., Coleman, R.A., 2002. Mitochondrial glycerol-3-phosphate acyltransferase-deficient mice have reduced weight and liver triacylglycerol content and altered

glycerolipid fatty acid composition. Mol. Cell. Biol. 22, 8204–8214. https://doi.org/10.1128/mcb.22.23.8204-8214.2002.
Han, H.S., Kang, G., Kim, J.S., Choi, B.H., Koo, S.H., 2016. Regulation of glucose metabolism from a liver-centric perspective. Exp. Mol. Med. 48, 1–10. https://doi.org/10.1038/emm.2015.122.
Huang, D.Y., Zhao, H.Q., Liu, C.P., Sun, C.X., 2014. Characteristics, sources, and transport of tetrabromobisphenol A and bisphenol A in soils from a typical e-waste recycling area in South China. Environ. Sci. Pollut. Res. 21, 5818–5826. https://doi.org/10.1007/s11356-014-2535-2.
Huang, M., Li, J., Xiao, Z., Shi, Z., 2020. Tetrabromobisphenol A and hexabromocyclododecane isomers in breast milk from the general population in Beijing, China: contamination levels, temporal trends, nursing infant's daily intake, and risk assessment. Chemosphere 244, 125524. https://doi.org/10.1016/j.chemosphere.2019.125524.
Jewison, T., Su, Y., Disfany, F.M., Liang, Y., Knox, C., MacIejewski, A., Poelzer, J., Huynh, J., Zhou, Y., Arndt, D., Djoumbou, Y., Liu, Y., Deng, L., Guo, A.C., Han, B., Pon, A., Wilson, M., Rafatnia, S., Liu, P., Wishart, D.S., 2014. SMPDB 2.0: big improvements to the small molecule pathway database. Nucleic Acids Res. 42, 478–484. https://doi.org/10.1093/nar/gkt1067.
Ji, H., Song, N., Ren, J., Li, W., Xu, B., Li, H., Shen, G., 2020. Metabonomics reveals bisphenol A affects fatty acid and glucose metabolism through activation of LXR in the liver of male mice. Sci. Total Environ. 703, 134681. https://doi.org/10.1016/j.scitotenv.2019.134681.
Jung, Y.-S., Lee, J., Seo, J., Hwang, G.-S., 2017. Metabolite profiling study on the toxicological effects of polybrominated diphenyl ether in a rat model. Environ. Toxicol. 32, 1262–1272. https://doi.org/10.1002/tox.22322.
Kamstra, J.H., Hruba, E., Blumberg, B., Janesick, A., Mandrup, S., Hamers, T., Legler, J., 2014. Transcriptional and epigenetic mechanisms underlying enhanced in vitro adipocyte differentiation by the brominated flame retardant bde-47. Environ. Sci. Technol. 48, 4110–4119. https://doi.org/10.1021/es405524b.
Kartsoli, S., Kostara, C.E., Tsimihodimos, V., Bairaktari, E.T., Christodoulou, D.K., 2020. Lipidomics in non-alcoholic fatty liver disease. World J. Hepatol. 12, 436–450. https://doi.org/10.4254/wjh.v12.i8.436.
Kim, U.J., Oh, J.E., 2014. Tetrabromobisphenol A and hexabromocyclododecane flame retardants in infant-mother paired serum samples, and their relationships with thyroid hormones and environmental factors. Environ. Pollut. 184, 193–200. https://doi.org/10.1016/j.envpol.2013.08.034.
Koh, E.J., Hwang, S.Y., 2019. Multi-omics approaches for understanding environmental exposure and human health. Mol. Cell. Toxicol. 15, 1–7. https://doi.org/10.1007/s13273-019-0001-4.
Lankova, D., Lacina, O., Pulkrabova, J., Hajslova, J., 2013. The determination of perfluoroalkyl substances, brominated flame retardants and their metabolites in human breast milk and infant formula. Talanta 117, 318–325. https://doi.org/10.1016/j.talanta.2013.08.040.
Li, A., Zhuang, T., Shi, W., Liang, Y., Liao, C., Song, M., Jiang, G., 2020. Serum concentration of bisphenol analogues in pregnant women in China. Sci. Total Environ. 707, 136100. https://doi.org/10.1016/j.scitotenv.2019.136100.
Li, H., Zhang, Z., Sun, Y., Wang, W., Xie, J., Xie, C., Hu, Y., Gao, Y., Xu, X., Luo, X., Mai, B., 2021. Tetrabromobisphenol A and hexabromocyclododecanes in sediments and biota from two typical mangrove wetlands of South China: distribution, bioaccumulation and biomagnification. Sci. Total Environ. 750, 141695. https://doi.org/10.1016/j.scitotenv.2020.141695.
Li, H., Zhang, Z., Zhao, Z.Z., 2019. Data-mining for processes in chemistry, materials, and engineering. Processes 7. https://doi.org/10.3390/pr7030151.
Liu, K., Li, J., Yan, S., Zhang, W., Li, Y., Han, D., 2016. A review of status of tetrabromobisphenol A (TBBPA) in China. Chemosphere 148, 8–20. https://doi.org/10.1016/j.chemosphere.2016.01.023.
Liu, M., Jia, S., Dong, T., Zhao, F., Xu, T., Yang, Q., Gong, J., Fang, M., 2020. Metabolomic and transcriptomic analysis of mcf-7 cells exposed to 23 chemicals at human-relevant levels: estimation of individual chemical contribution to effects. Environ. Health Perspect. 128. https://doi.org/10.1289/EHP6641 127008-1-127008–16.
Liu, Q., Shao, W., Weng, Z., Zhang, X., Ding, G., Xu, C., Xu, J., Jiang, Z., Gu, A., 2020. In vitro evaluation of the hepatic lipid accumulation of bisphenol analogs: a high-content screening assay. Toxicol. In Vitro 68, 104959. https://doi.org/10.1016/j.tiv.2020.104959.
Liu, Q.S., Sun, Z., Ren, X., Ren, Z., Liu, A., Zhang, J., Zhou, Q., Jiang, G., 2020. Chemical structure-related adipogenic effects of tetrabromobisphenol A and its analogues on 3T3-L1 preadipocytes. Environ. Sci. Technol. 54, 6262–6271. https://doi.org/10.1021/acs.est.0c00624.
Lu, L., Hu, J., Li, G., An, T., 2021. Low concentration tetrabromobisphenol A (TBBPA) elevating overall metabolism by inducing activation of the Ras signaling pathway. J. Hazard. Mater. 416, 125797. https://doi.org/10.1016/j.jhazmat.2021.125797.
Nakajima, A., Saigusa, D., Tetsu, N., Yamakuni, T., Tomioka, Y., Hishinuma, T., 2009. Neurobehavioral effects of tetrabromobisphenol A, a brominated flame retardant, in mice. Toxicol. Lett. 189, 78–83. https://doi.org/10.1016/j.toxlet.2009.05.003.
O'Dwyer, C., Yaworski, R., Katsumura, S., Ghorbani, P., Gobeil Odai, K., Nunes, J.R.C., LeBlond, N.D., Sanjana, S., Smith, T.T.K., Han, S., Margison, K.D., Alain, T., Morita, M., Fullerton, M.D., 2020. Hepatic choline transport is inhibited during fatty acid-induced lipotoxicity and obesity. Hepatol. Commun. 4, 876–889. https://doi.org/10.1002/hep4.1516.
Pang, Z., Chong, J., Zhou, G., De Lima Morais, D.A., Chang, L., Barrette, M., Gauthier, C., Jacques, P.É., Li, S., Xia, J., 2021. MetaboAnalyst 5.0: narrowing the gap between raw spectra and functional insights. Nucleic Acids Res. 49, W388–W396. https://doi.org/10.1093/nar/gkab382.
Parsons, A., Lange, A., Hutchinson, T.H., Miyagawa, S., Iguchi, T., Kudoh, T., Tyler, C.R., 2019. Molecular mechanisms and tissue targets of brominated flame retardants, BDE-47 and TBBPA, in embryo-larval life stages of zebrafish (Danio rerio). Aquat. Toxicol. 209, 99–112. https://doi.org/10.1016/j.aquatox.2019.01.022.
Possik, E., Al-Mass, A., Peyot, M.L., Ahmad, R., Al-Mulla, F., Madiraju, S.R.M., Prentki, M., 2021. New mammalian glycerol-3-phosphate phosphatase: role in β-cell,liver and adipocyte metabolism. Front. Endocrinol. (Lausanne) 12, 1–9. https://doi.org/10.3389/fendo.2021.706607.
Qu, G., Liu, A., Hu, L., Liu, S., Shi, J., Jiang, G., 2016. Recent advances in the analysis of TBBPA/TBBPS, TBBPA/TBBPS derivatives and their transformation products. TrAC - Trends Anal. Chem. 83, 14–24. https://doi.org/10.1016/j.trac.2016.06.021.
Qu, G., Yao, L., Wang, Yuanyuan, Shi, J., Liu, Yanna, Guo, H., Yang, X., Liu, Yaquan, Ma, J., Li, D., Wang, Z., Li, Z., Luo, Q., Fu, J., Zhang, Q., Wang, Yanxin, Jiang, G., 2021. Toxicity of tetrabromobisphenol a and its derivative in the mouse liver following oral exposure at environmentally relevant levels. Environ. Sci. Technol. 55, 8191–8202. https://doi.org/10.1021/acs.est.1c01726.
Riu, A., Grimaldi, M., le Maire, A., Bey, G., Phillips, K., Boulahtouf, A., Perdu, E., Zalko, D., Bourguet, W., Balaguer, P., 2011. Peroxisome proliferator-activated receptor γ is a target for halogenated analogs of bisphenol A. Environ. Health Perspect. 119, 1227–1232. https://doi.org/10.1289/ehp.1003328.
Sharma, V., Smolin, J., Nayak, J., Ayala, J.E., Scott, D.A., Peterson, S.N., Freeze, H.H., 2018. Mannose alters gut microbiome, prevents diet-induced obesity, and improves host metabolism. Cell Rep. 24, 3087–3098. https://doi.org/10.1016/j.celrep.2018.08.064.
Smith, C.A., Want, E.J., O'Maille, G., Abagyan, R., Siuzdak, G., 2006. XCMS: processing mass spectrometry data for metabolite profiling using nonlinear peak alignment, matching, and identification. Anal. Chem. 78, 779–787. https://doi.org/10.1021/ac051437y.
Tada, Y., Fujitani, T., Yano, N., Takahashi, H., Yuzawa, K., Ando, H., Kubo, Y., Nagasawa, A., Ogata, A., Kamimura, H., 2006. Effects of tetrabromobisphenol A, brominated flame retardant, in ICR mice after prenatal and postnatal exposure. Food Chem. Toxicol. 44, 1408–1413. https://doi.org/10.1016/j.fct.2006.03.006.
Thévenot, E.A., Roux, A., Xu, Y., Ezan, E., Junot, C., 2015. Analysis of the human adult urinary metabolome variations with age, body mass index, and gender by implementing a comprehensive workflow for univariate and OPLS statistical analyses. J. Proteome Res. 14, 3322–3335. https://doi.org/10.1021/acs.jproteome.5b00354.
Tian, J., Hong, Y., Li, Z., Yang, Z., Lei, B., Liu, J., Cai, Z., 2021a. Immunometabolism-modulation and immunotoxicity evaluation of perfluorooctanoic acid in macrophage. Ecotoxicol. Environ. Saf. 215, 112128. https://doi.org/10.1016/j.ecoenv.2021.112128.
Tian, J., Li, Z., Wang, L., Qiu, D., Zhang, X., Xin, X., Cai, Z., Lei, B., 2021b. Metabolic signatures for safety assessment of low-level cadmium exposure on human osteoblast-like cells. Ecotoxicol. Environ. Saf. 207, 111257. https://doi.org/10.1016/j.ecoenv.2020.111257.
van den Berghe, G., 1991. The role of the liver in metabolic homeostasis: implications for inborn errors of metabolism. J. Inherit. Metab. Dis. 14, 407–420. https://doi.org/10.1007/BF01797914.
Vuong, A.M., Braun, J.M., Sjödin, A., Calafat, A.M., Yolton, K., Lanphear, B.P., Chen, A., 2021. Exposure to endocrine disrupting chemicals (EDCs) and cardiometabolic indices during pregnancy: the HOME study. Environ. Int. 156. https://doi.org/10.1016/j.envint.2021.106747.
Wang, X.Y., Luo, J.P., Chen, R., Zha, X.Q., Pan, L.H., 2015. Dendrobium huoshanense polysaccharide prevents ethanol-induced liver injury in mice by metabolomic analysis. Int. J. Biol. Macromol. 78, 354–362. https://doi.org/10.1016/j.ijbiomac.2015.04.024.
Wang, Y., Niu, M., Jia, G.L.C., Li, R.S., Zhang, Y.M., Zhang, C.E., Meng, Y.K., Cui, H.R., Ma, Z.J., Li, D.H., Wang, J.B., Xiao, X.H., 2016. Untargeted metabolomics reveals intervention effects of total turmeric extract in a rat model of nonalcoholic fatty liver disease. Evid. Based Complement. Alternat. Med. 2016. https://doi.org/10.1155/2016/8495953.
Wishart, D.S., Feunang, Y.D., Marcu, A., Guo, A.C., Liang, K., Vázquez-Fresno, R., Sajed, T., Johnson, D., Li, C., Karu, N., Sayeeda, Z., Lo, E., Assempour, N., Berjanskii, M., Singhal, S., Arndt, D., Liang, Y., Badran, H., Grant, J., Serra-Cayuela, A., Liu, Y., Mandal, R., Neveu, V., Pon, A., Knox, C., Wilson, M., Manach, C., Scalbert, A., 2018. HMDB 4.0: the human metabolome database for 2018. Nucleic Acids Res. 46, D608–D617. https://doi.org/10.1093/nar/gkx1089.
Włuka, A., Woźniak, A., Woźniak, E., Michałowicz, J., 2020. Tetrabromobisphenol A, terabromobisphenol S and other bromophenolic flame retardants cause cytotoxic effects and induce oxidative stress in human peripheral blood mononuclear cells (in vitro study). Chemosphere. Elsevier Ltd. https://doi.org/10.1016/j.chemosphere.2020.127705.
Woeller, C.F., Flores, E., Pollock, S.J., Phipps, R.P., 2017. Thy1 (CD90) expression is reduced by the environmental chemical tetrabromobisphenol-A to promote adipogenesis through induction of microRNA-103. Toxicol. Sci. 157, 305–319. https://doi.org/10.1093/toxsci/kfx046.
Yang, R., Liu, S., Liang, X., Yin, N., Jiang, L., Zhang, Y., Faiola, F., 2021. TBBPA, TBBPS, and TCBPA disrupt hESC hepatic differentiation and promote the proliferation of differentiated cells partly via up-regulation of the FGF10 signaling pathway. Journal of Hazardous Materials. Elsevier B.V. https://doi.org/10.1016/j.jhazmat.2020.123341.
Yang, Yunjia, Li, Z., Zhang, J., Yang, Yi, Shao, B., 2014. Simultaneous determination of bisphenol A, bisphenol AF, tetrachlorobisphenol A, and tetrabromobisphenol A concentrations in water using on-line solid-phase extraction with ultrahigh-pressure liquid chromatography tandem mass spectrometry. Int. J. Environ. Anal. Chem. 94, 16–27. https://doi.org/10.1080/03067319.2013.853756.
Yin, J., Meng, Z., Zhu, Y., Song, M., Wang, H., 2011. Dummy molecularly imprinted polymer for selective screening of trace bisphenols in river water. Anal. Methods 3, 173–180. https://doi.org/10.1039/c0ay00540a.
Yousf, S., Sardesai, D.M., Mathew, A.B., Khandelwal, R., Acharya, J.D., Sharma, S., Chugh, J., 2019. Metabolic signatures suggest o-phosphocholine to UDP-N-acetylglucosamine ratio as a potential biomarker for high-glucose and/or palmitate exposure in pancreatic β-cells. Metabolomics 15. https://doi.org/10.1007/s11306-019-1516-3.
Yu, Y., Yu, Z., Chen, H., Han, Y., Xiang, M., Chen, X., Ma, R., Wang, Z., 2019. Tetrabromobisphenol A: disposition, kinetics and toxicity in animals and humans. Environ. Pollut. 253, 909–917. https://doi.org/10.1016/j.envpol.2019.07.067.
Zhu, A., Liu, P., Gong, Y., Li, M., Su, J., Liu, G., 2020. Residual levels and risk assessment of tetrabromobisphenol A in Baiyang Lake and Fuhe river,China. Ecotoxicol. Environ. Saf. 200, 110770. https://doi.org/10.1016/j.ecoenv.2020.110770.
Zhu, B., Zhao, G., Yang, L., Zhou, B., 2018. Tetrabromobisphenol A caused neurodevelopmental toxicity via disrupting thyroid hormones in zebrafish larvae. Chemosphere 197, 353–361. https://doi.org/10.1016/j.chemosphere.2018.01.080.